

CHARACTERIZATION OF NEUTRON LEAKAGE FIELD COMING FROM $^{18}\text{O}(\text{p},\text{n})^{18}\text{F}$ REACTION IN PET PRODUCTION CYCLOTRON

M. Schulc*, M. Kostal, E. Losa, J. Simon, F. Brijar, T. Czako, V. Rypar

Research Centre Rez, Husinec-Rez, Czechia

Z. Matej, F. Mravec¹, Masaryk University, Brno, Czechia

M. Antos, S. Vadjak, M. Cuhra², UJV Rez, Husinec-Rez, Czechia

F. Cvachovec³, University of Defence, Brno, Czechia

Abstract

The paper shows a new method for characterization of the secondary neutron field quantities, specifically a neutron spectrum leaking from ^{18}O enriched H_2O XL cylindrical target in IBA Cyclone 18/9 in the energy range of 1–15 MeV. This leakage spectrum is measured by stilbene scintillation detector in different places. The neutron spectra are evaluated from the measured proton recoil spectra using deconvolution through maximum likelihood estimation. A leakage neutron field is not only an interesting option for irradiation experiments due to a quite high flux, but also for a validation of high energy threshold reactions due to a relatively high average energy. The measured neutron spectra were compared with calculations in MCNP6 model by using TENDL-2017, FENDL-3, and default MCNP6 model calculations. TENDL-2017 and FENDL-3 libraries results differ significantly in the shape of the neutron spectrum for energies above 10 MeV while MCNP6 gives incorrect angular distributions. Activation measurements of the different neutron induced reactions support the characterization. The ^{18}F production yield is in a good agreement with TENDL-2017 proton library calculation within a respective uncertainties. The shape of the measured spectrum is also compared with the calculations with TALYS-1.9 using the different models.

INTRODUCTION

All experiments were performed using IBA Cyclone 18/9 accelerator (18 MeV for H^- , 9 MeV for D^- particle) which is located in UJV cyclotron laboratory. The most common radioisotope product of the facility is 2-fluoro-2-deoxy-D-glucose (FDG) labeled by ^{18}F which origins from $^{18}\text{O}(\text{p},\text{n})^{18}\text{F}$ reaction. Furthermore, it has the capacity to produce the other positron-emitting medical isotopes such as ^{11}C , ^{13}N , ^{15}O . The cyclotron is surrounded by a 4 m wide and 5.75 m long ferroconcrete shielding bunker as a biological shielding. The accelerator has 2 m in diameter and is centered to the shorter side and the same distance from the side wall.

Measurements were performed during irradiation (by 18 MeV protons) of 2.7 ml ^{18}O enriched water (minimal content of 98%). The water is placed in a niobium pin which is sealed by a Havar foil. Accelerator window is covered by a Ti foil. The current, generated by the proton beam on the target, was approximately 75 μA in case of the activation

experiments, while it was 0.92 μA in the case of neutron spectra measurements near target. The current was approximately 80 μA in the case of neutron and gamma spectra measured further from the target.

EXPERIMENTAL AND CALCULATION METHODS

The 10×10 mm stilbene scintillation detector was used for measuring neutron leakage spectra in the range of 1.0–14 MeV in the steps of 100 keV. Energy calibration was tested at LVR-15 reactor in Research centre Rez by means of a silicon filtered beam [1]. The efficiency calibration employs a measurement using a pure ^{252}Cf neutron source. This upgraded two-parameter spectrometric system NGA-01 [2, 3] is fully digitized and is now able to process up to 500 000 impulse responses per second. Pulse shape discrimination unit is used to distinguish the type of the detected particle by analyzing the pulse shape, while particle energy is evaluated from the integral of the whole response (energy integral). The pulse shape discrimination value is computed by the field-programmable gate array using an integration method which uses the comparison of the area delimited by part of a trailing edge of the measured response with the area delimited by the whole response. Then the neutron spectra are evaluated from the acquired recoiled proton spectra by means of deconvolution using Maximum Likelihood Estimation [4]. The substantial sources of uncertainty in the measurement were: an energy calibration uncertainty of 3–5%, an uncertainty in the efficiency crystal calibration factor 2.1%, and an uncertainty in the total emission of the neutron ^{252}Cf source 1.3%. Total measurement uncertainty, including statistical uncertainty and dispersion between measurements, is between approximately 2.4%–15% in the measured region.

In the case of activation experiments, the experimental reaction rates were derived from the gamma activities of irradiated samples. Irradiated samples were measured by means of a well-defined HPGe detector with verified geometry and efficiency calibration, for more details see [5]. The reaction rates were derived using the following formula:

$$q = C(T_m) \frac{\lambda \times k}{\epsilon \eta N} \frac{1}{1 - e^{-\lambda T_m}} \frac{1}{e^{\lambda \Delta T}} \frac{1}{1 - e^{-\lambda T_r}}, \quad (1)$$

where: q is the experimental reaction rate per atom per second, N is the number of target isotope nuclei, η is the detector efficiency, ϵ is gamma branching ratio, λ is the decay constant, ΔT is the time between the end of irradiation

* martin.schulc@cvrez.cz

and start of HPGe measurement, $C(T_m)$ is the measured number of counts, T_m is the time of measurement by HPGe, k is coincidence summing correction factor and T_{ir} is the time of irradiation.

Various types of samples were used, pure natural Ni, Fe and Al. The evaluated monitoring reactions were: $^{58}\text{Ni}(n,p)^{58}\text{Co}$, $^{60}\text{Ni}(n,p)^{60}\text{Co}$, $^{58}\text{Ni}(n,X)^{57}\text{Co}$, $^{54}\text{Fe}(n,p)^{54}\text{Mn}$, $^{54}\text{Fe}(n,\alpha)^{51}\text{Cr}$ and $^{27}\text{Al}(n,\alpha)^{24}\text{Na}$. The samples were placed and measured on the end cap of the HPGe detector. Very important is fact that the reaction $^{18}\text{O}(p,n)^{18}\text{F}$ produces gammas with very high energy up to 18 MeV. Those gammas can induce for instance (γ, n) reactions which have the same product as $(n,2n)$ reactions. Hence, the monitor reactions should be selected very carefully or contribution of parasitic reactions should be evaluated.

All calculations were performed using the MCNP6 Monte Carlo code [6] in coupled proton neutron transport mode. Default settings containing the Cascade-Exciton Model (CEM) is used for accelerated protons in the MCNP6 simulations. The CEM model, originally proposed in Dubna, incorporates all three stages of nuclear reactions: intranuclear cascade, pre-equilibrium, and equilibrium (or compound nucleus) [7] and [8]. In our case, mostly pre-equilibrium and equilibrium stages are applicable to our problem. The proton transport nuclear data libraries from TENDL-2017 [9] and FENDL-3 [10] proton transport libraries were also tested for mutual intercomparison. ENDF/B-VII.1 nuclear data library [11] was used for simulation of neutron interactions in structural materials and for $^{58}\text{Ni}(n,x)^{57}\text{Co}$ reaction. All other tested cross sections were calculated using dosimetric IRDFF-1.05 library [12]. It is worth noting that the structural components have special importance in the formation of the secondary neutron field. The lower part of the neutron spectrum arises from the backscattered neutrons from walls and structural components. The uncertainties in the calculated reaction rates were below 2%. The calculation uncertainties in the neutron fluence rate were about 2% in lower regions and 5-9% in upper regions.

Spectrum of outgoing neutrons from $^{18}\text{O}(p,n)^{18}\text{F}$ reaction was also calculated using TALYS-1.9 code [9] with different models. TALYS-1.9 is a system for the analysis and simulation of nuclear reactions. It can simulate nuclear reactions that involve neutrons, photons, protons, deuterons, tritons, $^3\text{He}^-$ and alpha particles, in the 1 keV–200 MeV energy range and for target nuclides of mass 12 and heavier.

RESULTS

Differential Neutron Spectra in Different Positions

As a first test, the reaction rate of production of ^{18}F isotope was investigated by measuring of its activity in a certified geometry, within 5% uncertainty. The TENDL-2017 cross section of $^{18}\text{O}(p,n)^{18}\text{F}$ reaction was used for comparison. The production rate of ^{18}F agrees well within uncertainties including uncertainty in enrichment and uncertainty in losses of enriched water in piping preceding activity measurement.

The neutron spectra were measured in different places of the cyclotron room using the stilbene detector. For real geometry, see Fig. 1. The places were following: position in the labyrinth (Labyrinth), position 1 (Position 1) and position 1 with Bi (Position 1 Bi filter). In the case of Position 1, the detector was surrounded by 30 cm of lead except top of the detector. In the case of position 1 with Bi, the additional 12 cm of Bi was placed in front of the top of the detector. The detector was always placed one meter above the ground. In these cases the proton current was approximately 80 μA . Results are shown in Fig. 2. The shape of spectra is very similar for energies higher than 3 MeV.

The neutron spectrum measured in position 80 cm from ^{18}O enriched H_2O target was compared with calculations using various incident proton nuclear data libraries, MCNP6 default calculations, FENDL-3 and TENDL-2017 libraries. The comparison is presented in Fig. 3. All calculations are comparable and reasonable up to 9 MeV. As can be seen, the calculations with TENDL-2017 differ significantly for energies higher than 9 MeV, the same can be stated for FENDL-3 calculations, however the discrepancy is smaller. The most reasonable agreement with experiment is in the case of MCNP6 calculation. The C/E-1 comparison is presented in Fig. 4. It is clear that the discrepancy in the 2–6 MeV interval is 2–3 times higher than the related uncertainty and in for energies higher than 10 MeV, the difference can be up to five times higher the respective uncertainty. More details can be found in [13].

The gamma spectrum was measured by stilbene detector in the labyrinth, see Fig. 5. The gamma spectrum is very hard, thus one have to be aware of gamma induced reactions in the case of evaluation of some monitor reactions.

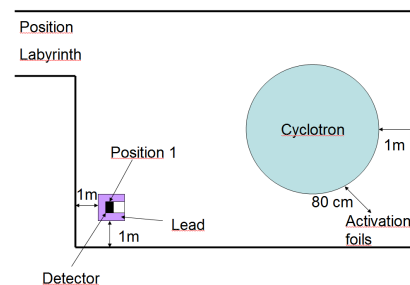


Figure 1: Geometry of the measurements.

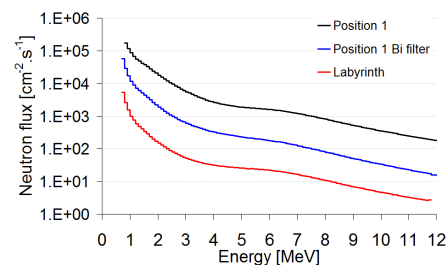


Figure 2: Measured neutron spectra in different places.

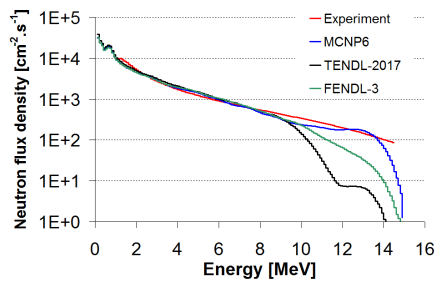


Figure 3: Comparison of measured and calculated neutron spectrum 80 cm from cyclotron end.

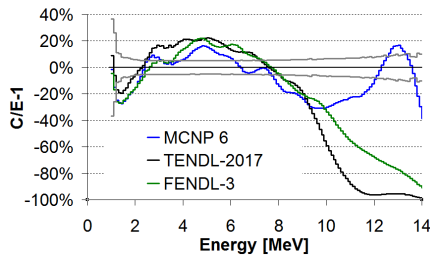


Figure 4: C/E-1 comparison of calculated and measured neutron spectrum 80 cm from cyclotron end.

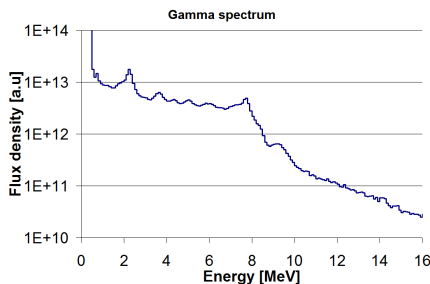


Figure 5: Measured gamma spectrum in the labyrinth.

Reaction Rates Measurement

Table 1 shows comparison of measured and calculated reaction rates by means of Calculation(C) to Experiment(E) ratios. The samples for irradiation were placed in distance of 80 cm in cyclotron vertical axis from the target, i.e. in the same place as neutron spectra were measured. The cross sections for reactions under study except $^{58}\text{Ni}(n,X)^{57}\text{Co}$ were taken from IRDFF-1.05 library because these reactions are dosimetric and are validated in different neutron spectra. In the case of FENDL-3 calculations, the results are not satisfactory for all reactions.

TENDL-2017 performs better with very good agreement for $^{58}\text{Ni}(n,p)^{58}\text{Co}$ and $^{54}\text{Fe}(n,p)^{54}\text{Mn}$ reactions. All other reaction rates are reproduced very poorly. Concerning default MCNP6 model results, the agreement is satisfactory and overall best from these three calculations with maximum discrepancy almost 20%.

Table 1: C/E-1 of the Measured Reaction Rates 80 cm from the Cyclotron End

Reaction	MCNP6	FENDL-3	TENDL-2017
$^{58}\text{Ni}(n,p)^{58}\text{Co}$	13.4%	23.1%	-2.8%
$^{54}\text{Fe}(n,p)^{54}\text{Mn}$	19.8%	29.4%	1.4%
$^{54}\text{Fe}(n,\alpha)^{51}\text{Cr}$	-5.0%	-20.6%	-49.3%
$^{60}\text{Ni}(n,p)^{60}\text{Co}$	-7.3%	-18.9%	-47.0%
$^{27}\text{Al}(n,\alpha)^{24}\text{Na}$	-13.2%	-34.1%	-62.2%
$^{58}\text{Ni}(n,X)^{57}\text{Co}$	-2.5%	-73.2%	-96.3%

Comparison with TALYS-1.9

Figure 6 shows comparison of shapes of measured and TALYS-1.9 calculated neutron spectra. Generally, the agreement is satisfactory for neutron energies higher than 2 MeV. The lower energies are influenced by the scattered neutrons by walls and structural components in the case of experiment. In the case of simulation with no compound nucleus, the agreement is the worst. The reasonable agreement is also achieved with disabled the pre-equilibrium reaction mechanism. The best agreement is achieved with default calculation using widthmode 0, it corresponds to the case where no width fluctuation corrections in compound nucleus are implemented, i.e. calculations use pure Hauser-Feshbach model.

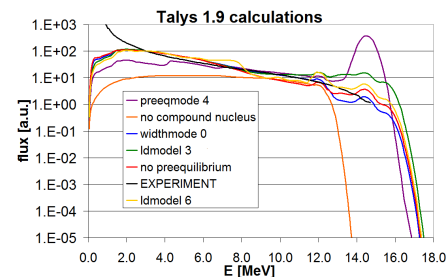


Figure 6: Comparison of measured spectrum with ones calculated using TALYS-1.9.

CONCLUSION

The leakage neutron field of the ^{18}F production reaction was measured at IBA Cyclone 18/9 cyclotron with XL cylindrical target for the first time. This technique can be used in principle in any cyclotron for measuring neutron evaporation spectra up to 15 MeV. The employed proton libraries show significant discrepancies, thus they are not suitable for a precise description of the secondary neutron field to be used as a scientific instrument. The TENDL-2017 and FENDL-3 libraries differ significantly in the shape of the spectrum in the high-energy tail, whereas MCNP6 default model is incorrect in the angular distribution. However, the calculations of the ^{18}F production yields, the TENDL-2017 cross section gives a very good results with discrepancy about 3 % which is comparable with the respective uncertainties. Either neutron and photon spectrum can be effectively characterized

Content from this work may be used under the terms of the CC BY 3.0 licence (© 2019). Any distribution of this work must maintain attribution to the author(s), title of the work, publisher, and DOI

using a stilbene scintillation detector and the flux with neutron activation analysis performed with suitable samples. However, the reactions to be under study must be carefully selected due to the influence of the parasitic photonuclear reactions. Concerning TALYS-1.9 calculations, the shape of the spectrum is reproduced very well. The best agreement is achieved with the calculations using pure Hauser-Feshbach model.

ACKNOWLEDGEMENTS

Presented results were obtained with the use of the infrastructure Reactors LVR-15 and LR-0, which is financially supported by the Ministry of Education, Youth and Sports Czech Republic – project LM2015074 and – project LQ1603 Research for SUSEN. This work has been realized within the SUSEN Project (established in the framework of the European Regional Development Fund (ERDF) in project CZ.1.05/2.1.00/03.0108 and of the European Structural Funds and Investment Funds (ESIF), Czech Republic in the project CZ.02.1.01/0.0/0.0/15_008/0000293), which is financially supported by the Ministry of Education, Youth and Sports, Czech Republic – project LM2015093 Infrastructure SUSEN.

REFERENCES

- [1] M. Kostal, J. Soltes, L. Viererbl, *et al.*, “Measurement of neutron spectra in a silicon filtered neutron beam using stilbene detectors at the LVR-15 research reactor”, *Appl. Rad. and Isot.*, vol. 128, pp. 41–48, Oct. 2017. doi:10.1016/j.apradiso.2017.06.026
- [2] M. Veskrna, Z. Matej, F. Mravec, V. Prenosil, F. Cvachovec, and M. Kostal, “Digitalized two parametric system for gamma/neutron spectrometry”, in *Proc. 18th Topical Meeting of the Radiation Protection and Shielding Division of ANS*, Knoxville, TN USA, Sep. 2014. <https://pdfs.semanticscholar.org/f6dc/a5a72824d730d0a54a145097fd2cdace6acc.pdf>
- [3] Z. Matej, *Digitalization of spectrometric system for mixed field of radiation*, Saarbrücken, Germany: LAP LAMBERT Academic Publishing, Sep. 2014. ISBN 978-3-659-59970-5.
- [4] J. Cvachovec and F. Cvachovec, “Maximum likelihood estimation of a neutron spectrum and associated uncertainties”, *Advances in Military Technology*, vol. 3, no. 2, Dec. 2008. https://www.researchgate.net/publication/267992287_Maximum_Likelihood_Estimation_of_a_Neutron_Spectrum_and_Associated_Uncertainties
- [5] M. Kostal, M. Schulc, V. Rypar, *et al.*, “Validation of zirconium isotopes (n,g) and (n,2n) cross sections in a comprehensive LR-0 reactor operative parameters”, *Appl. Rad. and Isot.*, vol. 128, pp. 92–100, Oct. 2017. doi:10.1016/j.apradiso.2017.06.023
- [6] T. Goorley *et al.*, “Initial MCNP6 release overview”, *Nucl. Technol.*, vol. 180, pp. 298–315, Aug. 2012. doi:10.13182/NT11-135
- [7] K. K. Gudima, S. G. Mashnik, and V. D. Toneev, “Cascade-exciton model of nuclear reactions”, *Nucl. Phys. A*, vol. 401(2), pp. 401–329, Jun. 1983. doi:10.1016/0375-9474(83)90532-8
- [8] A. C. Kraan, “Range verification methods in particle therapy underlying physics and Monte Carlo modeling”, *Front. Oncol.*, vol. 5, 2015. doi:10.3389/fonc.2015.00150
- [9] A. J. Koning and D. Rochman, “Modern nuclear data evaluation with the TALYS code system”, *Nucl. Data Sheets*, vol. 113, pp. 2841–2934, Dec. 2012. doi:10.1016/j.nds.2012.11.002
- [10] R. A. Forrest *et al.*, “FENDL-3 library summary documentation”, Report INDC(NDS)-628, 2013. <https://40.68.46.107/publications/indc/indc-nds-0628.pdf>
- [11] M. B. Chadwick, M. Herman, P. Oblozinsky, *et al.*, “ENDF/B-VII.1: Nuclear data for science and technology: Cross sections, covariances, fission product yields and decay data”, *Nucl. Data Sheets*, vol. 112, pp. 2887–2996, Dec. 2011. doi:10.1016/j.nds.2011.11.002
- [12] R. Capote, K. I. Zolotarev, V. G. Pronyaev, and A. Trkov, “Updating and extending the IRDF-2002 dosimetry library”, *J. ASTM Int. (JAI)*- 9, Issue 4, pp. 1-9, Apr. 2012. doi:10.1520/JAI104119
- [13] M. Kostal *et al.*, “The methodology of characterization of neutron leakage field from PET production cyclotron for experimental purposes”, *Nucl. Instrum. Methods Phys. Res., Sect. A*, vol. 942, art. no. 162374, 2019. doi:10.1016/j.nima.2019.162374